Journal of Nepal Mathematical Society (JNMS)
ISSN: 2616-0153 (Print), 2616-0161 (Online)
Vol. 7, Issue 2, 2024 (Dec.): 40-49
DOI: https://doi.org/10.3126/jnms.v7i2.73103

Research Article
Received Date: July 20, 2024
Accepted Date: Dec. 19, 2024
Published Date: Dec. 29, 2024

A Mathematical Modeling of Blood Flow Through Artery with Bell-Shaped Stenosis

Kedar Nath Chhatkuli[1,2], Pushpa Nidhi Gautam[3], Jeevan Kafle[1,*]

[1]Institute of Science and Technology, Central Department of Mathematics, Tribhuvan University, Kathmandu, Nepal
[2]Department of Mathematics, Amrit Campus, Tribhuvan University, Kathmandu, Nepal
[3]Department of Mathematics, Patan Multiple Campus, Tribhuvan University, Lalitpur, Nepal
[*]Correspondence to: Jeevan Kafle, Email: jeevan.kafle@cdmath.tu.edu.np

Abstract: *This study investigates the effect of bell-shaped stenosis on blood flow within arteries, a critical factor in understanding cardiovascular health. Using the Navier-Stokes equation in cylindrical polar coordinates, we derive analytical solutions for key hemodynamic parameters, including velocity, pressure, pressure drop ratio, and wall shear stress. Numerical integration is applied to explore the dynamics of pressure drop, and shear stress ratios within the stenotic region and various flow parameters are investigated and analyzed in this work considering blood as a Newtonian fluid. Given the heightened risk posed by bell-shaped stenosis in conditions like ischemic heart disease and stroke, this research offers valuable insights into the behavior of blood flow in stenotic arteries. The findings contribute to the development of advanced analytical tools and therapeutic strategies in cardiology and bio-fluid mechanics, enhancing our ability to manage and treat cardiovascular diseases.*

Keywords: Bell-shaped stenosis, Numerical integration, Volumetric flow rate, Pressure drop, Shear stress

1 Introduction

Stenosis is a pathological restriction of an artery due to fat and cholesterol deposition inside arteries lumen involving narrowing or constriction of the inner surface of the arteries [6, 20]. Different types of stenosis may occur within arteries. Stenosis in arteries is the most common. Aortic stenosis, which resists the blood flow from ventricle to aorta by narrowing the heart valves, can be serious and potentially fatal. The major categories of stenosis are: aortic stenosis, tricuspid stenosis, pulmonary stenosis, mitral stenosis, renal artery stenosis, spinal stenosis, and tracheal stenosis [4]. Aortic stenosis is the most common type of stenosis which narrows the aortic valve and then restricts the blood flow from the ventricle into the aorta. Balloon Angioplasty is one of the most common surgeries applied in widening the narrowed stenosed blood

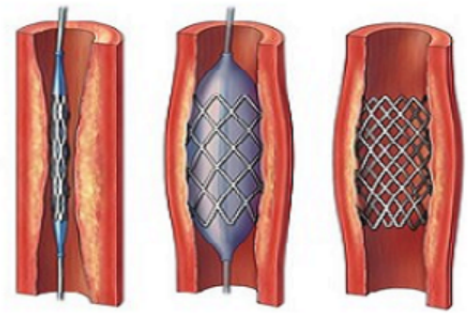

Figure 1: Balloon Angioplasty [9].

vessel. The human cardiovascular system, is a closed network of heart, lungs, arteries, veins, and capillaries. Arteries transport oxygen-rich blood, but any fat intrusion in their walls may partially or fully block the blood flow, causing oxygen deficiency. Intra-vascular atherosclerotic plaque, known as stenosis, narrows the arteries and causes arterial disorders. The disruption of blood flow causes angina pectoris, cerebral stroke, heart attacks, and strokes [12, 14, 20]. Cardio vascular diseases (CVDs), affecting both men and women,

are disorders of blood vessels and heart. Blood that is rich in oxygen is transported by arteries throughout the body, making the cardiovascular network essential for life.

Nutrition, blood constituent chemistry, and genetics play major roles in atherosclerosis development. Beginning early in life and worsening with age, stenosis impedes circulation, causing strokes, heart failure, and paralysis [4, 13]. It often occurs in curved sections of coronary, carotid, abdominal, and pelvic arteries, especially at low shear rates and high viscosity. Blood pressure increases as stenosis develops to maintain blood flow [3]. According to World Health Organization (WHO) report 2023, nearly one-third of all deaths ($\approx$7.9 million people annually) are due to CVDs [23]. Stenosis weakens the heart and causes ischemic heart disease (IHD) by narrowing arteries and reducing blood flow. With 16% of all deaths, this is the biggest cause of death worldwide. In 2020, IHD deaths rose by 122.47% from 2019, the highest increase among non-communicable diseases [7, 23]. Stenosis is a key factor in CVDs like IHD, stroke, and chronic obstructive pulmonary disease. Due to the high risk associated with stenosis, studying blood flow in stenotic arteries is crucial. Previous research has made significant contributions to understanding and treating CVDs caused by stenosis. The condition poses a major challenge due to its impact on blood flow, leading to serious health risks [23]. These are among the top three global killers according to the WHO's 2020 report [7, 23]. Severe stenosis, particularly when it narrows arteries to nearly the radius, can block blood flow, leading to fatal outcomes.

Lee and Fung [8] studied blood flow in a cylindrical coordinate system of the Navier-Stokes equations. Young [21] defined the geometry of stenosis using the cosine function and computed flow parameters to initiate the mathematical investigation of blood flow in an artery with mild stenosis. Different flow parameters were analyzed using analytical solutions by Pokharel et al. [11]. Srivastav and Agnihotri [19] explored blood flow in a catheterized artery with bell-shaped stenosis, assuming blood behaves as a power-law fluid. Goutam et al. [5] calculated the effect of increasing stenosis on flow parameters, considering blood as a non-Newtonian fluid. Shah and Kumar [15], and Srivastava et al. [20] contributed to understanding flow disturbances caused by stenosis.

According to Bugliarello and Sevilla [1], blood viscosity and deformability depend on hematocrit and vary significantly with shear rate and artery size. The impact of a non-Newtonian power-law blood fluid model on flow characteristics was studied by Srivastav and Agnihotri [17]. Young and Tsai [22] described steady flow in vitro tests, investigating important hydrodynamic variables such as separation, turbulence, and pressure drop. Cokelet [2] studied the rheology of human blood. Sohail et al. [16] studied blood flow through arteries with four distinct stenotic regions: triangular, trapezoidal, overlapping, and composite. These works have made significant strides in understanding the complex processes controlling blood flow in stenotic arteries, which will greatly impact the development of innovative treatments for cardiovascular disease.

Bell-shaped stenosis poses unique challenges due to its potential to be more dangerous than other types of stenosis. The distinct geometry of this stenosis can significantly affect blood flow, leading to complications in cardiovascular health. In this study, the analytical investigation of hemodynamic parameters, including velocity, pressure, and wall shear stress, in the bell-shaped stenotic region has been carried out, which is crucial for advancing medical science. By applying numerical integration to model the blood flow within the artery's stenotic segment, we aim to provide a comprehensive understanding of how these parameters interact. This research not only enhances our knowledge of the complexities associated with bell-shaped stenosis but also offers valuable insights for developing more effective treatments for blood flow-related diseases. The advanced analytical approach used in this work could pave the way for more accurate diagnostic tools and therapeutic strategies in managing cardiovascular conditions [18]. This research focuses on the dynamics of blood flow in bell-shaped stenosis, which may be more dangerous than other types. The findings could inform treatments for patients with this condition and aid in advanced blood flow studies [18, 19].

2 Methods

2.1 Model equation

The blood flow in arteries can be modeled considering it as flow inside a cylinder. Let r and p stand for the artery radius and pressure drop respectively. Components of the velocities along radial, angular and axial directions are u^r, u^θ and u^z respectively. The Navier–Stokes equations (N-S equations) of continuity and the equations of motion in cylindrical coordinate system are [10].

$$\frac{\partial u^r}{\partial r} + \frac{u^r}{r} + \frac{1}{r}\frac{\partial u^\theta}{\partial \theta} + \frac{\partial u^z}{\partial z} = 0, \tag{1}$$

$$\rho\left(\frac{\partial u^r}{\partial t} + u^r\frac{\partial u^r}{\partial r} + \frac{u^\theta}{r}\frac{\partial u^r}{\partial \theta} - \frac{(u^\theta)^2}{r} + u^z\frac{\partial u^r}{\partial z}\right) = -\frac{\partial p}{\partial r} + \mu\left[-\frac{u^r}{r^2} + \frac{1}{r}\frac{\partial}{\partial r}\left(r\frac{\partial u^r}{\partial r}\right) + \frac{1}{r^2}\frac{\partial^2 u^r}{\partial \theta^2} + \frac{2}{r^2}\frac{\partial u^\theta}{\partial \theta} + \frac{\partial^2 u^r}{\partial z^2}\right] + g_r \tag{2}$$

$$\rho\left(\frac{\partial u^\theta}{\partial t} + u^r\frac{\partial u^\theta}{\partial r} + \frac{u^\theta}{r}\frac{\partial u^\theta}{\partial \theta} + \frac{u^r u^\theta}{r} + u^z\frac{\partial u^\theta}{\partial z}\right) = -\frac{\partial p}{\partial \theta} + \mu\left[-\frac{u^\theta}{r^2} + \frac{1}{r}\frac{\partial}{\partial r}\left(r\frac{\partial u^\theta}{\partial r}\right) + \frac{1}{r^2}\frac{\partial^2 u^\theta}{\partial \theta^2} - \frac{2}{r^2}\frac{\partial u^r}{\partial \theta} + \frac{\partial^2 u^\theta}{\partial z^2}\right] + g_\theta \tag{3}$$

$$\rho\left(\frac{\partial u^z}{\partial t} + u^r\frac{\partial u^z}{\partial r} + \frac{u^\theta}{r}\frac{\partial u^z}{\partial \theta} + u^z\frac{\partial u^z}{\partial z}\right) = -\frac{\partial p}{\partial z} + \mu\left[\frac{1}{r}\frac{\partial}{\partial r}\left(r\frac{\partial u^z}{\partial r}\right) + \frac{1}{r^2}\frac{\partial^2 u^z}{\partial \theta^2} + \frac{\partial^2 u^z}{\partial z^2}\right] + g_z. \tag{4}$$

We assume that in the axisymmetric flow, $u^\theta = 0$ and that u^r, u^z, and p are independent of θ. For the steady flow of blood, viscosity μ and density ρ are considered to be constant. The gravity components g_r, g_θ and g_z are supposed to have negligible effect in the blood flow through artery and are not included. Then momentum balance equation (4) reduces to

$$\frac{\mu}{r}\frac{\partial}{\partial r}\left(r\frac{\partial u^z}{\partial r}\right) = \frac{\partial p}{\partial z} \tag{5}$$

If we suppose $u^z = u(r)$, and $P = -\partial p/\partial z$ from Kapur [7], equations (5) reduces to,

$$-P\frac{r}{\mu} = \frac{\partial}{\partial r}\left(r\frac{\partial u}{\partial r}\right) \tag{6}$$

Initially we have supposed $\partial u/\partial r = 0$ at $r = 0$, again R_0 and R are the radii of the artery in non-stenotic and in stenotic region respectively then,

$$u = \begin{cases} 0 \text{ at } r = R, & |z| \le z_0, \\ 0 \text{ at } r = R_0, & |z| > z_0. \end{cases} \tag{7}$$

Integrating the equation (6) with respect to r,

$$r\frac{\partial u}{\partial r} = -P(z)\frac{r^2}{2\mu} + C(z). \tag{8}$$

Using the boundary conditions we get $C(z) = 0$ and integrating (8),

$$u = -\frac{Pr^2}{4\mu} + D(z). \tag{9}$$

Using the boundary condition $u = 0$ at $r = R$, gives $D(z) = PR^2/4\mu$. It follows the velocity distribution as

$$u = \frac{P}{4\mu}(R^2 - r^2). \tag{10}$$

2.2 Geometry of bell-shaped stenosis

Examine the axisymmetric blood flow via a bell-shaped stenosis of length $2z_0$ in an artery, located as shown in Figure 2. According to Srivastava et al. [18], the geometry of bell-shaped stenosis in the artery wall segment, is expressed as follows:

$$R(z) = \begin{cases} R_0 - \delta \exp\left(\frac{-w^2\epsilon^2 z^2}{R_0^2}\right), & |z| \le z_0, \\ R_0, & |z| > z_0. \end{cases} \tag{11}$$

where $R(z)$ is radius of the stenosed portion located at the axial distance z from the center 0 of the

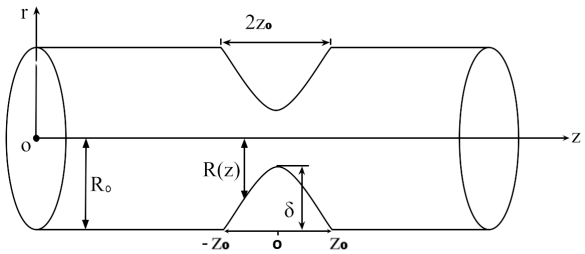

Figure 2: Representative sketch for artery and bell-shaped stenosis.

segment, R_0 is radius of the arterial segment in the non-stenotic region, δ is depth of stenosis at the throat, w is a parametric constant, ϵ is the relative length of the constriction given as $\epsilon = \frac{R_0}{z_0}$

2.3 Volumetric flow rate

The volumetric flow rate via the cylindrical tube can be obtained as[7],

$$Q = \int_0^R 2\pi\, r\, u\, dr = \frac{2P\pi}{4\mu} \int_0^R (rR^2 - r^3)\, dr = \frac{\pi P}{8\mu} R^4. \tag{12}$$

2.4 Pressure drop and its ratio

The pressure term from equation (12) is

$$P(z) = \frac{8\mu Q}{\pi R^4} \tag{13}$$

After integrating (13), the pressure drop in the stenosed portion is obtained as

$$\triangle P = \int_{-z_0}^{z_0} P(z)\, dz = \frac{8\mu\, Q}{\pi} \int_{-z_0}^{z_0} \frac{1}{R^4} dz \tag{14}$$

For bell-shaped stenosis, on using equation (11) in equation (14) for $-z_0 \le z \le z_o$, the pressure drop across the stenosed length is

$$\triangle P = \frac{8\mu\, Q}{\pi} \int_{-z_0}^{z_0} \left[R_0 - \delta \exp\left(\frac{-w^2\epsilon^2 z^2}{R_0^2}\right)\right]^{-4} dz \tag{15}$$

When there is no stenosis, $\delta = 0$, but then the pressure drop without stenosis becomes

$$(\triangle P)_0 = \frac{16\mu z_0 Q}{\pi R_0^4} \tag{16}$$

The ratio of the pressure drop with stenosis to the pressure drop without stenosis is

$$\frac{\triangle P}{(\triangle P)_0} = \frac{R_0^4}{2z_0}\int_{-z_0}^{z_0} \frac{1}{\left[R_0 - \delta \exp\left(\frac{-w^2\epsilon^2 z^2}{R_0^2}\right)\right]^4} dz \tag{17}$$

which is written as,

$$\frac{\triangle P}{(\triangle P)_0} = \frac{R_0^4}{2z_0}\int_{-z_0}^{z_0} f(z)\, dz, \tag{18}$$

where

$$f(z) = \frac{1}{\left[R_0 - \delta\, \exp\left(\frac{-w^2\epsilon^2 z^2}{R_0^2}\right)\right]^4} \tag{19}$$

Using Simpson's 3/8 rule for definite integral, the equation (18) becomes:

$$\frac{\triangle P}{(\triangle P)_0} = \frac{3hR_0^4}{16z_0}\left[f(z_o)+3\sum_{i=1,4,7,\ldots}^{n-2} f(z_i)+3\sum_{i=2,5,8,\ldots}^{n-1} f(z_i)+2\sum_{i=3,6,9,\ldots}^{n-3} f(z_i)+f(z_n)\right] \tag{20}$$

where n is the number of sub-intervals in the interval $[-z_0, z_0]$ and the length of each sub-interval $h = \frac{2z_0}{n}$.

2.5 Shear stress

The stress across the stenosis surface is given by [12]

$$\tau = \frac{PR}{2}$$

Using equation (13)

$$\tau = \frac{8\mu Q}{\pi R^4}\frac{R}{2} = \frac{4\mu Q}{\pi R^3} \tag{21}$$

If there is no stenosis inside the artery wall, $\delta = 0$ and the shear stress without stenosis τ_0 is given by

$$\tau_0 = \frac{4\mu Q}{\pi R_0^3} \tag{22}$$

2.6 Shear stress ratio

The ratio of shear stress with stenosis to the shear stress without stenosis is

$$\frac{\tau}{\tau_0} = \left(\frac{R_0}{R}\right)^3 \tag{23}$$

Using (11) in the interval $[-z_0, z_0]$, we get the ratio of shear stress as follows:

$$\frac{\tau}{\tau_0} = \left[\frac{R_0}{R_0 - \delta \exp\left(\frac{-w^2\epsilon^2 z^2}{R_0^2}\right)}\right]^3 \tag{24}$$

At the throat, we have $z = 0$ and $R = R_0 - \delta$ then

$$\frac{\tau}{\tau_0} = \left[\frac{R_0}{R_0 - \delta}\right]^3 \tag{25}$$

3 Results and Discussions

Different hemodynamic parameters are used to plot the graphs such as $R_0 = 3$ mm; $w = 0.5$ mm s^{-1}; $P = 90$ mm of Hg; $z_0 = 1$ mm; $\delta = 2$ mm; if not mentioned in the graphs.

3.1 Velocity profile

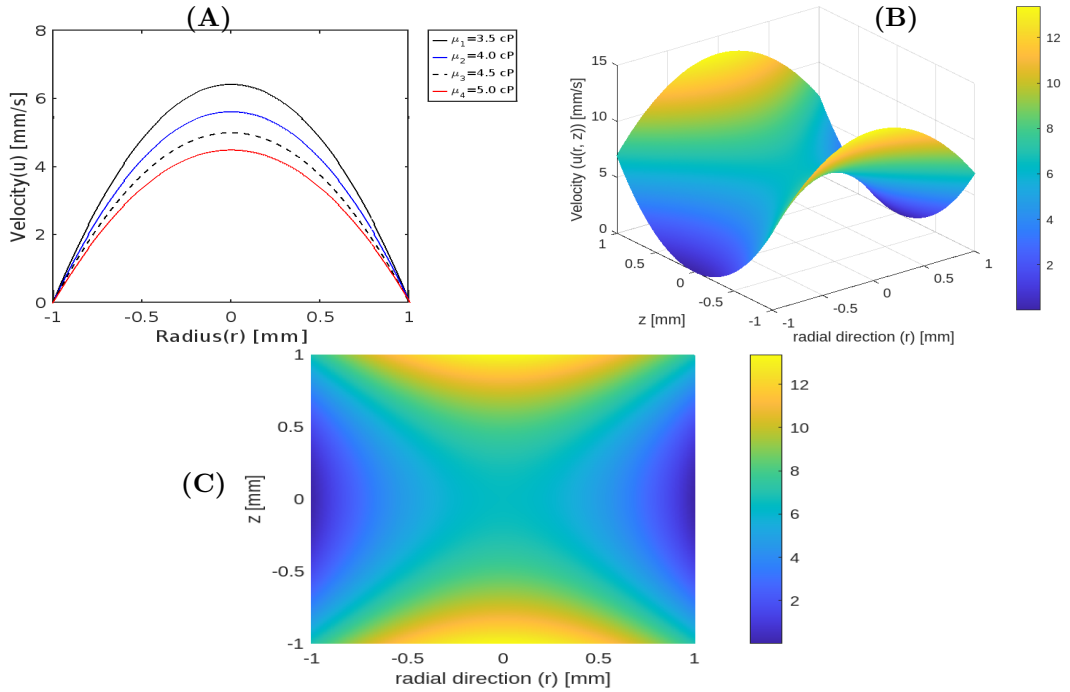

Figure 3: Velocity Profiles of blood flow in bell-shaped stenosis **(A)** by varying viscosity μ with respect to radial direction (r) at $z = 0$, **(B)** varying radial direction (r) and axial direction (z) for viscosity 3.5 cP and **(C)** contour plot for $u(r, z)$.

Figure 3 depicts the velocity profile (u) for equation (10). From Figure 3, the velocity is maximum at the axis (i.e., at $r = 0$) of the artery. The velocity is minimum and equal to 0 at $r = 1$ and $z = 0$. Fig. 3**(A)**, for $z = 0$, displays that the maximum velocity are approximately equal to 6.43 mm s^{-1}, 5.63 mm s^{-1}, 5.00 mm s^{-1}, and 4.50 mm s^{-1}, for viscosity (in cP) equal to 3.5, 4.0, 4.5, and 5.0, respectively, at $r = 0$. At $\mu = 3.5$ cP, the velocity attains the values 6.43 mm s^{-1} at $r = 0.0$ mm, 6.03 mm s^{-1} at $r = 0.25$mm, 4.82 mm s^{-1} at $r = 0.5$, 2.81 mm s^{-1} at $r = 0.75$ mm and 0 at $r = 1$ mm. Similar nature, but less value of velocity is observed for higher viscosity value. When μ takes the value 4.0 cP, the velocity takes 5.63 mm s^{-1} at $r = 0.0$ mm, 5.27 mm s^{-1} at $r = 0.25$mm ,4.22 mm s^{-1} at $r = 0.5$, 2.46 mm s^{-1} at $r = 0.75$ mm and 0 at $r = 1$ mm. Furthermore, as μ takes the values of 4.5 cP, the velocity takes 5.00 mm s^{-1} at $r = 0.0$ mm, 4.69 mm s^{-1} at $r = 0.25$mm ,3.75 mm s^{-1} at $r = 0.5$, 2.19 mm s^{-1} at $r = 0.75$ mm and 0 at $r = 1$ mm.

Figure 3**(B)** & **(C)** are the graphs of $u(r, z)$ for $\mu = 3.5$, indicates that minimum velocity is zero at $(r, z) = (1, 0)$; this means the velocity is zero obeying no-slip condition at the apex wall of stenosis. At the axis of the artery i.e., at $r = 0$, the velocity attains the maximum values 6.43 mm s^{-1} at $z = 0$mm, 6.83 mm s^{-1} at $z = 0.25$mm, 8.08 mm s^{-1} at $z = 0.5$mm, 10.24 mm s^{-1} at $z = 0.75$mm, 13.37 mm s^{-1} at $z = 1$mm. These results obtained from Fig. 3 are: (i) the velocity is maximum at the axis (i.e., $r = 0$ for each z) of the artery then goes on decreasing as r increases and reduces to zero at the boundary obeying the no- slip condition; (ii) velocity is minimum at $z = 0$ for each r; (iii) it decreases with upward concavity for $z \in [-1, 0)$ and increases with upward concavity for each $z \in (0, 1]$; (iv) velocity increases to the left and right of the throat of the stenosis i.e., u varies directly to the stenosis radius (R). Thus the above results conclude that the velocity of blood flow through bell-shaped stenosis is maximum at the axis of the artery,

minimum (i.e. equal to 0) at the wall of the stenosis; it goes on increasing pattern as radius of artery (r) increases. Velocity profiles can be analyzed for other values of δ too.

3.2 Volumetric flow rate (VFR)

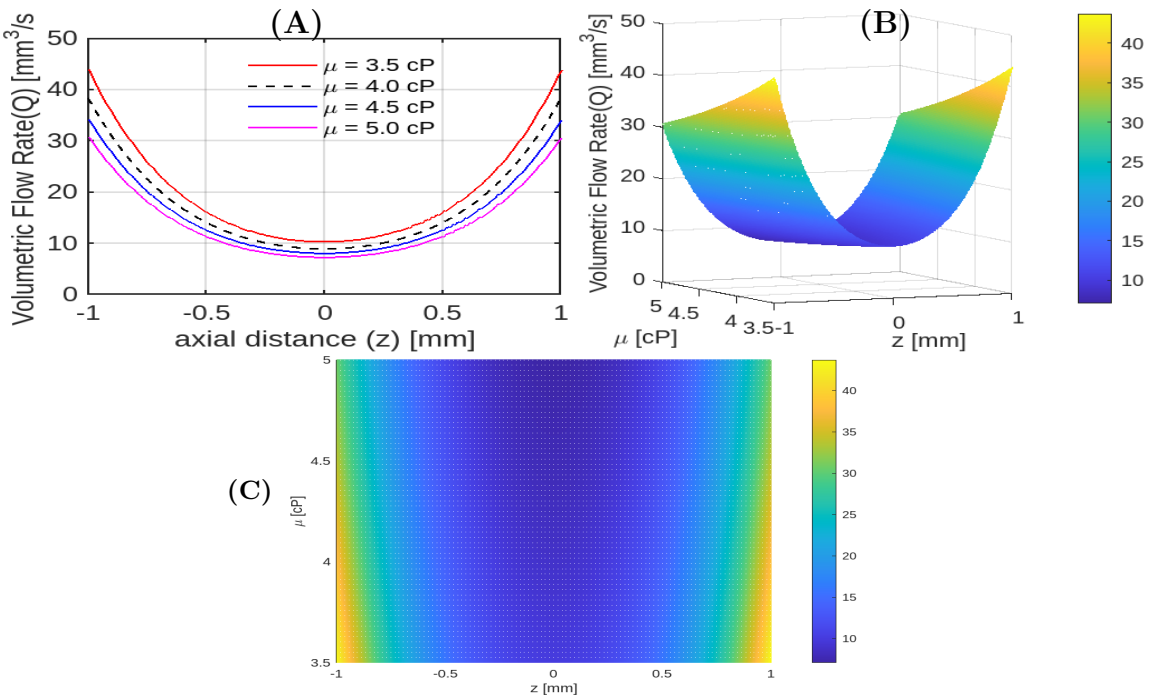

Figure 4: Volumetric flow rates **(A)** $Q(z)$ for various values of viscosity μ and **(B) & (C)** $Q(z, \mu)$.

Figure 4, plotted for equation (12), displays the relation between rate of volumetric flow(Q) along the axial distance (z) for various viscosities (μ). Here z varies from -1 to 1. At $\mu = 3.5$, the values of Q are $43.71\,\mathrm{mm^3\,s^{-1}}$ for $z = 1\,\mathrm{mm}$, $15.95\,\mathrm{mm^3\,s^{-1}}$ for $z = 0.5\,\mathrm{mm}$, and $10.10\,\mathrm{mm^3\,s^{-1}}$ for $z = 0\,\mathrm{mm}$. Also, at $\mu = 5.0$, the values of Q are $30.60\,\mathrm{mm^3\,s^{-1}}$ for $z = 1\,\mathrm{mm}$, $11.17\,\mathrm{mm^3\,s^{-1}}$ for $z = 0.5\,\mathrm{mm}$, and $7.07\,\mathrm{mm^3\,s^{-1}}$ for $z = 0\,\mathrm{mm}$. At $z = 0$, Q takes minimum values of approximately $10.10\,\mathrm{mm^3\,s^{-1}}$, $8.84\,\mathrm{mm^3\,s^{-1}}$, $7.85\,\mathrm{mm^3\,s^{-1}}$ and $7.07\,\mathrm{mm^3\,s^{-1}}$ for μ equals to 3.5, 4.0, 4.5, and, 5.0 respectively. At $z = 1$, Q takes maximum values approximately $43.71\,\mathrm{mm^3\,s^{-1}}$, $38.25\,\mathrm{mm^3\,s^{-1}}$, $34.00\,\mathrm{mm^3\,s^{-1}}$ and $30.60\,\mathrm{mm^3\,s^{-1}}$ for μ equals to 3.5, 4.0, 4.5, and, 5.0 respectively.

The conclusions drawn from Figures 4**(A)**, 4**(B)**, and 4**(C)** are: (i) Q gives the minimum values at the throat (i.e.$z = 0$) of stenosis and maximum value at the origin and ending of stenosis (i.e. at $z = 1$) for each value of μ; (ii) Q decreases as μ increases; (iii) for each μ, Q decreases with upward concavity in $z = [-1, 0]$ and increases with upward concavity in $z = [0, 1]$; iv) moving towards the maximum height of stenosis, the volumetric flow rate decreases, causing the inadequate blood supply.

3.3 Ratio of pressure drop

The ratio of pressure drops ($\frac{\Delta P}{(\Delta P)_0}$) for various heights of stenosis (δ mm) is depicted in the graph displayed in Fig. 5 for varying radius of artery. Initially the ratio has been obtained 1 irrespective of the size of the artery. When stenosis reaches the height 0.5 mm pressure drop ratio increases to 2.87, 2.27, 1.95, and 1.76 for respective radii 2 mm, 2.3 mm, 2.6 mm, and 3 mm. The ratio raises by 11.31 %, 5.42 %, 3.39 %, and 2.42 % when height of stenosis increases from 0 mm to 1 mm for radii of artery (R_0) 2 mm, 2.3 mm, 2.6 mm, and 3.0 mm respectively. We can conclude that with the increment of blockage the pressure drop ratio also picks up and if with higher blockage and smaller artery size the risk of penetration also increases due to

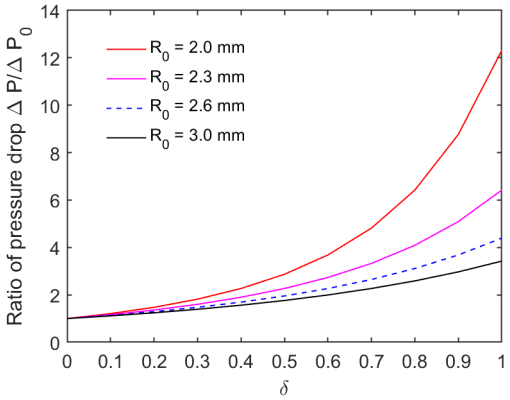

Figure 5: The ratio of pressure drop with respect to height of stenosis (δ) $[mm]$.

the over exposure of pressure on the artery wall. Graphs are plotted for fixing R_0 equal to 2 mm, 2.3 mm, 2.6 mm, and 3.0 mm. The figure illustrates that the ratio of pressure drops is always 1 if there is no stenosis ($\delta = 0$). For $R_0 = 3$ mm, when δ bears the values 0.4 mm, 0.8 mm, and 1.0 mm then the ratio of pressure drops take the values 1.56, 2.58, and 3.42 respectively. Thus we conclude that the ratio of pressure drop is an increasing function of height of stenosis.

3.4 Ratio of shear stress

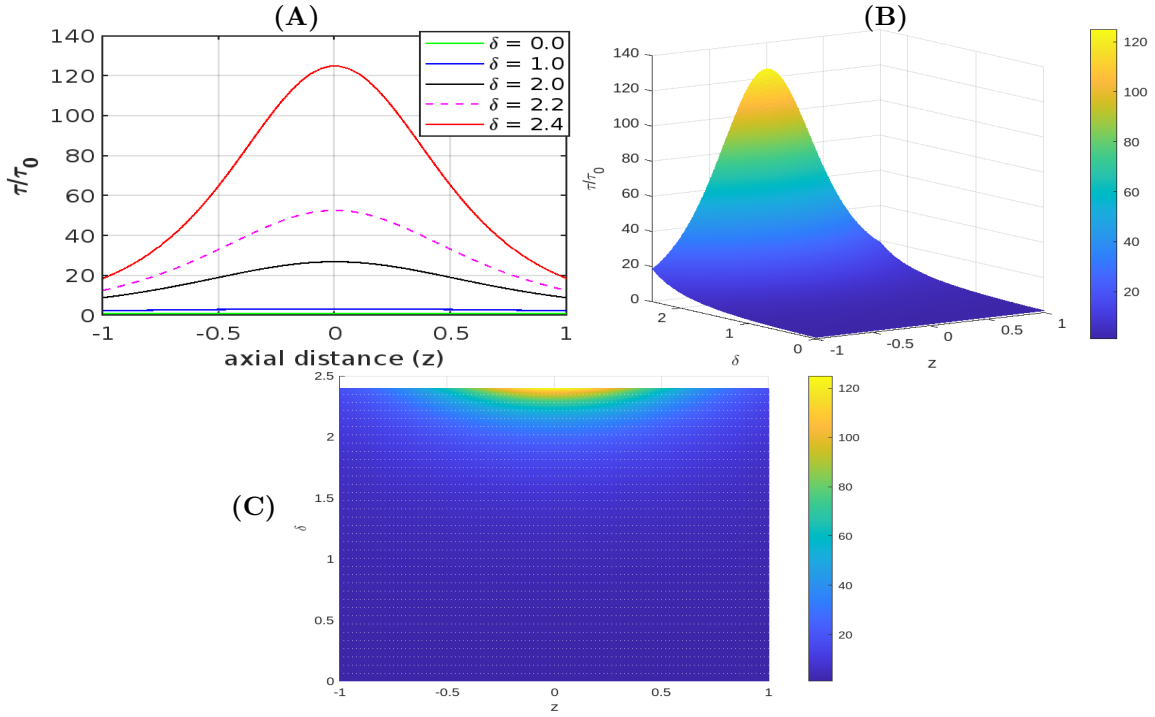

Figure 6: Shear stress ratio **(A)** with respect to axial distance (z) and; **(B) & (C)** with respect to axial distance (z) and height of stenosis (δ).

Figures 6**(A)**, 6**(B)** and, 6**(C)**, the plot of equation (24), analyze the trend of the shear stress ratio ($\frac{\tau}{\tau_0}$) on varying z and δ. When $\delta = 0$, then $\frac{\tau}{\tau_0} = 1$ for all $z \in [-1, 1]$. For $\delta = 1$ mm, $\frac{\tau}{\tau_0}$ takes the values approximately 2.46, 3.09, and 3.38 at z equals to 1, 0.5, and 0 respectively. For $\delta = 2.4$ mm, $\frac{\tau}{\tau_0}$ takes the

values approximately 18.67, 65.19, and 125.00 when z equals to 1, 0.5 and 0 respectively. When height of stenosis (δ) reaches 2.2 mm from 2.0 mm, the maximum value of $\frac{\tau}{\tau_0}$ reaches 52.72 from 27.00. Similarly, when height of stenosis (δ) reaches to 2.4 mm from 2.2 mm, the maximum value of $\frac{\tau}{\tau_0}$ reaches to 125.00 from 52.72; this shows that when (δ) increases by 9.09% from 2.2 mm, then the maximum value of $\frac{\tau}{\tau_0}$ increases by 137.06%, leading to severe situation. Thus, the conclusions, from the results of the graphs, are: (i) the shear stress ratio is unity when there is no stenosis; (ii) the shear stress ratio is maximum at the throat of stenosis (i.e. at $z = 0$) and minimum at the extremities of stenosis (i.e., at $z = 1$); (iii) the shear stress ratio goes on increasing for each $z \in [-1, 0)$ and goes on decreasing for each $z \in (0, 1]$; (iv) for $\delta \in (0, 1]$, there is a small change in $\frac{\tau}{\tau_0}$ i.e., when δ is less than $33\frac{1}{3}\%$ of R_0 under the consideration may not be a severe situation; for $\delta > 1$, the value of $\frac{\tau}{\tau_0}$ increases rapidly; and when δ exceeds $66\frac{2}{3}\%$ of R_0 under the consideration results in exponentially rapid growth of $\frac{\tau}{\tau_0}$ which causes severe situation in a patient, and thus the medical doctors must handle the case urgently and very carefully.

4 Conclusion

The analysis of axisymmetric, laminar, and steady flow in a bell-shaped stenosis artery is explored in this article considering blood as a Newtonian fluid. Analytical solutions were derived for the parameters of blood flow via a bell-shaped stenotic artery, including velocity profile, volumetric flow rate, pressure, pressure drop, and shear stress. The study found that blood velocity decreases with increasing viscosity and is highest at the center of the artery, dropping to zero at the wall. Volumetric flow rate decreases with higher viscosity and stenosis. Additionally, the ratio of pressure drop increases with stenotic height, indicating a higher risk of artery wall penetration due to increased pressure. Shear stress ratio increases with artery radius. When δ is less than $33\frac{1}{3}\%$ of R_0 under the consideration may not be severe situation but it becomes severe when δ exceeds $66\frac{2}{3}\%$ of R_0 under the consideration due to exponential growth of $\frac{\tau}{\tau_0}$. These findings offer valuable insights into the intricate dynamics of blood flow in a bell shaped stenosed arteries. This result may be useful for medical and bio-engineering field, especially in the prediction and management of cardiovascular diseases.

References

[1] Bulgliarello, G., and Sevilla, J., 1970, Velocity distributed and other characteristic of steady and pulsatile blood flow in fine glass tube, *Biorheology*, 7, 85-107, PMID: 5484335. DOI: https://doi.org/10.3233/bir-1970-7202

[2] Cokelet, G. R., 1972, *The Rheology of Human Blood*, Y. C. Fung (Eds.), Prentice-Hall, Englewood Cliffs.

[3] Diwakar, C., and Kumar, S., 2016, Effects of axially symmetric stenosis on the blood flow in an artery having mild stenosis, *International Journal of Mathematics Trends and Technology*, 35(3), 163-167. DOI: https://doi.org/10.14445/22315373/IJMTT-V35P522

[4] Gautam, P. N., Pokharel, C., Phaijoo, G. R., Kattel, P., and Kafle, J., 2023, Effect of Increasing Stenosis over Time on Hemodynamics *BIOMATH*. https://doi.org/10.55630/j.biomath.2023.10.067

[5] Goutam, D., Agrawal, B., and Kumar, S., 2023, Mathematical Modeling of Non-Newtonian Blood Flow through Arterial Stenosis, *Samdarshi* 16(4), ISSN: 2581- 3986.

[6] Kafle, J., Gaire, H. R., Pokheral, P. R., and Kattel, P., 2022, Analysis of blood flow through curved artery with mild stenosis, *Mathematical Modeling and Computing*, 9(2), 217–225. DOI: https://doi.org/10.23939/mmc2022.02.217

[7] Kapur, J. N., 1985, *Mathematical Models in Biology and Medicine*, Affiliated East-West Press Pvt. Ltd., New Delhi, India.

[8] Lee, J. S., and Fung, Y. C., 1970, Flow in locally constricted tube at low Reynalds Number, *Journal of Applied Mechchanics*, 37, 9-16. DOI: https://doi.org/10.1115/1.3408496

[9] Marker, K., 2015, Improving Post-Heart Attack Stent Surgery. https://www.labroots.com/trending/cardiology/2103/improving-post-heart-attack-stent-surgery.

[10] Menon, S. H., Rao, R. A., Mathew, J., and Jayaprakash, J., 2021, Derivation of Navier–Stokes equation in rotational frame for engineering flow analysis, *International Journal of Thermofluids*. DOI: https://doi.org/10.1016/j.ijft.2021.100096

[11] Pokharel, C., Gautam, P. N., Tripathee, S. T., Bhatta, C. R., and Kafle, J., 2022, Analysis of flow parameters in blood flow through mild stenosis *Nepalese Journal of Zoology*, 6(2), 39–44. https://doi.org/10.3126/njz.v6i2.51882

[12] Pokhrel, P. R., Kafle, J., Kattel, P., and Gaire, H. P., 2020, Analysis of blood flow through artery with mild stenosis, *Journal of Institute of Science and Technology*, 25(2), 33-38, DOI: https://doi.org/10.3126/jist.v25i2.33732

[13] Ponalagusamy, R., and Machi, R., 2020, A study of an two-layered (K.L-Newtonian) model of blood flow in an artery with six types of mild stenoses, *Applied Mathematics and computation*, 367, 124767, ISSN: 0096-3003. DOI: https://doi.org/10.1016/j.amc.2019.124767

[14] Tripathee, S. T., and Kafle, J., 2023, Analysis of Effect of Hemodynamic Parameters on Two Layered Blood Flow in a Mild Stenosed Artery, *Nepali Math. Sc. Report Journal*, 40(1- 2), 93-105. DOI: https://doi.org/10.3126/nmsr.v40i1-2.61505

[15] Shah, S. R., and Kumar, R., 2020, Mathematical modeling of blood flow with suspension of nanoparticle through a tapered artery with blood clot, *Frontiers in Nanotechnology*, 2:596475. DOI: https://doi.org/10.3389/fnano.2020(596475)

[16] Sohail, N., Salman, A., Anber, S., Nevzat, A., Hassan, A. G., Sayed, M. E., 2023, Numerical computations of blood flow through stenosed arteries via CFD tool OpenFOAM, *Alexandria Engineering Journal*, 69, 613-637. DOI: https://doi.org/10.1016/j.aej.2023.02.005

[17] Srivastav, R. K., and Agnihotri, A. K., 2014, Non-Newtonian Power-Law Blood Fluid Flow through a Bell-Shaped Stenosis in Artery, *Journal of Multidisciplinary Scientific Research*, 2(4), 15-19.

[18] Srivastava, V. P., Tandon, M., and Srivastav, R. K., 2012, A macroscopic two-phase blood flow through a bell-shaped stenosis in an artery with permeable wall, *Applications and Applied Mathematics* 7(1), 37-51.

[19] Srivastav, R. K., and Agnihotri, A. K., 2014, Blood Flow through a Bell-Shaped Stenosis in Catheterized Arteries, *Journal of Multidisciplinary Scientific Research*, 2(4), 15-19.

[20] Srivastava, V. P., Rastogi, R., Vishnoi, R., 2010, A two-layered suspension blood flow through an overlapping stenosis, *Computers and Mathematics with Applications*, 60(3), 432-441, https://doi.org/10.1016/j.camwa.2010.04.038.

[21] Young, D., 1968, Effect of a time-dependent stenosis on flow through a tube, *Journal of Engineering and Industrial Transactions*, ASME, 90, 248-254. DOI: https://doi.org/10.1115/1.3604621

[22] Young, D. F., and Tsai, F. Y., 1973, Flow Characteristics in Models of Arterial Stenosis—Steady Flow, *Journal of Biomechanics*, 6(4), 395-410. https://doi.org/10.1016/0021-9290(73)90099-7

[23] WHO. *The top 10 causes of death*. https://www.who.int/news-room/fact-sheets/detail/cardiovascular-diseases-(cvds)